

Energy transfer and trapping in photosystem I reaction centers from cyanobacteria

LISA DiMAGNO*†‡, CHI-KIN CHAN*†§, YIWEI JIA*†, MATTHEW J. LANG*†, JOHN R. NEWMAN*†, LAURENS METS‡, GRAHAM R. FLEMING*†, AND ROBERT HASELKORN*†¶

Departments of *Chemistry and ‡Molecular Genetics and Cell Biology, †James Franck Institute, and ¶Center for Photochemistry and Photobiology, The University of Chicago, 920 East 58 Street, Chicago, IL 60637

Contributed by Robert Haselkorn, December 22, 1994

ABSTRACT A mutant strain of the cyanobacterium *Synechocystis* 6803, *ToIE4B*, was constructed by genetic deletion of the protein that links phycobilisomes to thylakoid membranes and of the CP43 and CP47 proteins of photosystem II (PSII), leaving the photosystem I (PSI) center as the sole chromophore in the photosynthetic membranes. Both intact membrane and detergent-isolated samples of PSI were characterized by time-resolved and steady-state fluorescence methods. A decay component of ≈ 25 ps dominates (99% of the amplitude) the fluorescence of the membrane sample. This result indicates that an intermediate lifetime is not associated with the intact membrane preparation and the charge separation in PSI is irreversible. The decay time of the detergent-isolated sample is similar. The 600-nm excited steady-state fluorescence spectrum displays a red fluorescence peak at ≈ 703 nm at room temperature. The 450-nm excited steady-state fluorescence spectrum is dominated by a single peak around 700 nm without 680-nm "bulk" fluorescence. The experimental results were compared with several computer simulations. Assuming an antenna size of 130 chlorophyll molecules, an apparent charge separation time of ≈ 1 ps is estimated. Alternatively, the kinetics could be modeled on the basis of a two-domain antenna for PSI, consistent with the available structural data, each containing ≈ 65 chlorophyll molecules. If excitation can migrate freely within each domain and communication between domains occurs only close to the reaction center, a charge separation time of 3–4 ps is obtained instead.

Understanding of the photochemical reaction center known as photosystem I (PSI) has been greatly increased with the publication of its 6-Å x-ray structure (1). However, questions concerning the light-harvesting and trapping mechanisms of this complex remain, particularly since the positions of only half of the chlorophyll (Chl) molecules have been assigned. The PSI center is a membrane-bound, multiprotein complex that catalyzes the light-driven transport of electrons from reduced plastocyanin or cytochrome c_{553} to soluble ferredoxin or flavodoxin (2, 3). The complex is known to contain 10 or 11 polypeptides, about 100 Chl molecules, and 10–15 β -carotenes. The major reaction center proteins are called PsaA, PsaB, and PsaC, having molecular masses of 83, 83, and 9 kDa, respectively. PsaA and PsaB are disposed symmetrically in the membrane and share bonding to segment P700 itself, the primary electron donor which may be a Chl a dimer, and to A_0 , a monomeric Chl-a; A_1 , a phylloquinone (vitamin K); and F_x , a Fe_4-S_4 center. The two remaining Fe_4-S_4 centers, F_A and F_B , are bound to PsaC.

We are interested in how energy transfer and trapping occur in PSI. The elementary transfer time (≈ 150 – 300 fs) in the PSI core antenna of a PSI-only mutant of *Chlamydomonas reinhardtii* has been determined in a fluorescence up-conversion

experiment (4). This single-step transfer time very closely approximates a previous estimate using a simple two-color lattice model (5). Energy transfer from antenna to reaction center pigments is believed to occur by an incoherent hopping mechanism (6, 7), although strong coupling between Chls may also be important.

A detailed understanding of the structural relationships between antenna and reaction centers is a prerequisite to describing the processes that regulate excitation transfer and photochemical trapping reactions. To take account of inhomogeneous broadening and multiple spectral types in PSI, a multicolor random model with a few pigments that absorb above 700 nm (red pigments) was proposed (8). This model is consistent with the rather complex observed wavelength dependence of fluorescence decay in PSI at low temperatures (9). It was also concluded, based on the simulation, that red pigments are necessary to interpret the temperature and wavelength dependence of fluorescence decay at low temperatures (8, 9). This conclusion is supported by the direct observation of red fluorescence (the fluorescence peaks to the red of 700 nm) of PSI at room temperature (10). One of the key assumptions in the simulations (8) is the average distance (11.5 Å) between Chls, which is consistent with the x-ray structure (1). The simulation results indicated a nearly single exponential decay of the fluorescence at room temperature, implying that spectral equilibration occurs on a time scale faster than the trapping time. In this case, steady-state fluorescence with multiple-spectral types is likely to give a single major peak as observed by Holzwarth *et al.* (10). However, a recent study by Woolf *et al.* (11) gave a very different spectrum in which two emitting pools (680- and 703-nm peaks) were observed at room temperature, and the number of red pigments (703 nm) was estimated to be 8–11. This observation is reexamined here.

In time-resolved fluorescence experiments on photosystem II (PSII)-deficient *C. reinhardtii* mutants, the kinetic complexity of the decays depended on the number of peripheral Chls associated with the core antenna (9). The shortest decay component arises from excitation trapping in the PSI core. Fluorescence decay studies of detergent-isolated PSI reaction centers indicate variability, depending on the isolation procedure, the polypeptide and pigment composition, spectral properties, and core antenna size (5, 12–14). To study better-characterized samples, we constructed a cyanobacterial mutant containing PSI (≈ 130 Chls per P700) as its only chlorophyll-containing protein. Recently, Hastings *et al.* (15) reported measurements on a similar PSII-less mutant, in which ≈ 100 Chls per P700 were found. In this paper, we present a

Abbreviations: Chl, chlorophyll; PSI and PSII, photosystems I and II. ‡Present address: Biology Division, California Institute of Technology, Pasadena, CA 91125.

§Present address: Laboratory of Chemical Physics, National Institute of Diabetes and Digestive and Kidney Diseases, National Institutes of Health, Bethesda, MD 20892.

¶To whom reprint requests should be addressed.

The publication costs of this article were defrayed in part by page charge payment. This article must therefore be hereby marked "advertisement" in accordance with 18 U.S.C. §1734 solely to indicate this fact.

different analysis of the results and their implications. In particular, we relate our results to lattice-model simulations and propose a two-domain antenna model for PSI.

MATERIALS AND METHODS

Bacterial Cultures and Growth Conditions. Cultures of *Synechocystis* 6803 were grown in liquid mineral medium, BG-11, as described by Herdman *et al.* (16) but with twice the concentration of sodium nitrate. Mutant strains were grown in the same medium supplemented with 5 mM glucose and the antibiotics spectinomycin (20 $\mu\text{g/ml}$), streptomycin (10 $\mu\text{g/ml}$), kanamycin (30 $\mu\text{g/ml}$), and chloramphenicol (7 $\mu\text{g/ml}$). Cultures were grown at 30°C under 3000-lux illumination in a growth chamber containing an atmosphere with 2% CO_2 .

Construction of TolE4B. Construction of the *Synechocystis* 6714 *apcE*-inactivation plasmid pLDES² and *Synechocystis* 6803 *psbB*-inactivation plasmid pLRBS² has been described (17). These plasmids were used to introduce deletions, by transformation and homologous recombination, into the *Synechocystis* 6803 TOL1357 strain already lacking the *psbC* gene (18). Selection was first made for cells that could grow in the presence of spectinomycin and streptomycin (deletion/insertion to produce the strain TolE lacking the *apcE* gene) and then kanamycin (second deletion/insertion to produce the strain TolE4B, additionally lacking the *psbB* gene). The TolE4B strain cannot make CP43, CP47, or the linker protein that joins phycobilisomes to the thylakoid membrane (17).

Thylakoid Membrane and PSI Particle Isolation. Thylakoid membranes were prepared by established procedures (17). PSI particles were isolated from the TolE4B thylakoid membranes by Aida Pascual, using a procedure modified from one described for *Chlamydomonas* (5). The membrane preparation was dissolved in 1% Triton X-100/50 mM Tris chloride, pH 7.4/10 mM ascorbate to give a Chl concentration of 1.3 mg/ml in a final volume of 5 ml. The resulting suspension was centrifuged for 10 min at 27,000 $\times g$, and the supernatant was loaded on a 10-ml hydroxylapatite column at 4°C and then washed successively with 50-ml portions of 10 mM sodium phosphate (pH 7.0) containing 1 mM ascorbate (buffer A), buffer A containing 0.1% Triton X-100, and buffer A lacking Triton X-100. Finally, the particles were eluted with 50 ml of 200 mM sodium phosphate, pH 7.0/5 mM ascorbate/0.025% Triton X-100. These particles can be stored at -80°C. The hydroxylapatite column was prepared on the day of use by standard procedures (12). Triton X-100 (Bio-Rad) was purified by borohydride reduction following deionization on brominated Dowex 50X8-100 resin (19). The purified detergent was stored under argon at -80°C.

Spectroscopy. P700 content was estimated by measuring the light-induced absorbance changes at 697 nm with respect to 725 nm, using a differential extinction coefficient of 64 $\text{mM}^{-1}\cdot\text{cm}^{-1}$ (12, 20). The concentration of Chl-a was obtained either by direct measurement of absorbance at 667 nm and use of the extinction coefficient 60 $\text{mM}^{-1}\cdot\text{cm}^{-1}$ or by extraction of chlorophyll from the membranes with 80% (vol/vol) acetone. Steady-state fluorescence emission spectra were measured at 293 K with a Spex Fluorolog-2 fluorimeter in the front-face emission configuration.

Fluorescence decay measurements were made with a time-correlated single-photon counting apparatus (21). The excitation pulses (≈ 10 ps, 630 or 665 nm) were generated from a cavity-dumped DCM [4-(dicyanomethylene)-2-methyl-6-(*p*-dimethylaminostyryl)-4*H*-pyran] dye laser synchronously pumped by a mode-locked argon ion laser (514.5 nm). The pulse repetition rate was 3.8 MHz. The single-pulse intensity was adjusted to $\approx 10^{11}$ photons per cm^2 . Annihilation is not expected to occur at this intensity level for an ≈ 130 -chlorophyll antenna.

Simulations. Simulations of the steady-state fluorescence peak position and the decay kinetics were performed by using the model of ref. 8 with the following changes: (i) a three-dimensional lattice model replaced the two-dimensional model used previously; (ii) the lineshapes of the single-site absorption and fluorescence spectra were calculated as before and used directly in the energy-transfer dynamics (no Gaussian approximation to the lineshape was made); and (iii) Förster rates were calculated by numerical integration. Although a random model with two red pigments close to the reaction center was used, this model and a model with all pigments randomly distributed around the reaction center gave very similar results at room temperature. The spectral components, with our independently assigned amplitudes in parentheses, are those proposed by van Grondelle *et al.* (22): 703(4), 700(2), 693(8), 684(12), 680(32), 677(32), 671(32), and 666(8) nm. We determined the amplitudes by fitting the absorption spectrum of the membrane sample and assuming constant oscillator strength for all Chls. The fluorescence Stokes shift for each spectral type was taken to be 12 nm (22) except for the red pigments and the reaction center dimer. We used a 14-nm Stokes shift for the latter two spectral types (22). The unit lattice length was chosen as 10–11 Å in agreement with values of 8–15 Å taken from the PSI crystal structure. The charge-transfer rate was varied to compare the overall decay rate with the experimental results.

RESULTS

The blue-green color of cyanobacteria is due to phycobiliproteins that function principally as the light-harvesting antenna for PSII. The mutations introduced to create the strain TolE4B delete the linker protein required to anchor phycobilisomes to the thylakoid membrane and CP-43 and CP-47, the principal Chl-containing proteins of PSII. In the absence of the latter two proteins, the reaction center core proteins, D1 and D2, do not assemble in the membrane (18). Thus, the only Chl-containing proteins expected to remain in the thylakoids of mutant TolE4B are those of PSI. The absorption spectrum of TolE4B membranes is shown in Fig. 1. The principal absorbance peak is at 678 nm with a shoulder at 665 nm, both attributable to Chl. The small peak at 625 nm is due to some residual phycocyanin that contaminates the membrane preparation. There is also a shoulder below 500 nm attributable to carotenoids.

Steady-state fluorescence emission spectra recorded for membranes prepared from TolE4B are shown in Fig. 2. Excitation at 600 nm is shown in Fig. 2 *Upper*; excitation at 570 nm gives virtually the same spectrum. The principal peak is at 648 nm, which is at a much shorter wavelength than the absorption maximum of Chl-a and therefore cannot be due to Chl fluorescence. This peak is probably due to the trace of

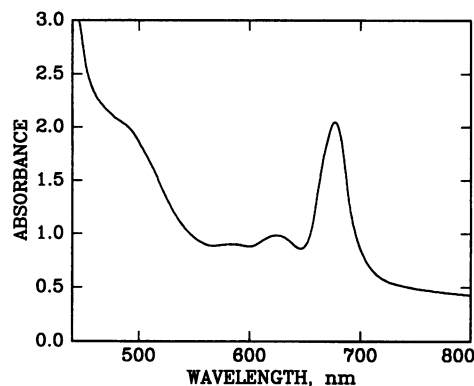


FIG. 1. Absorption spectrum of TolE4B membranes suspended in buffer.

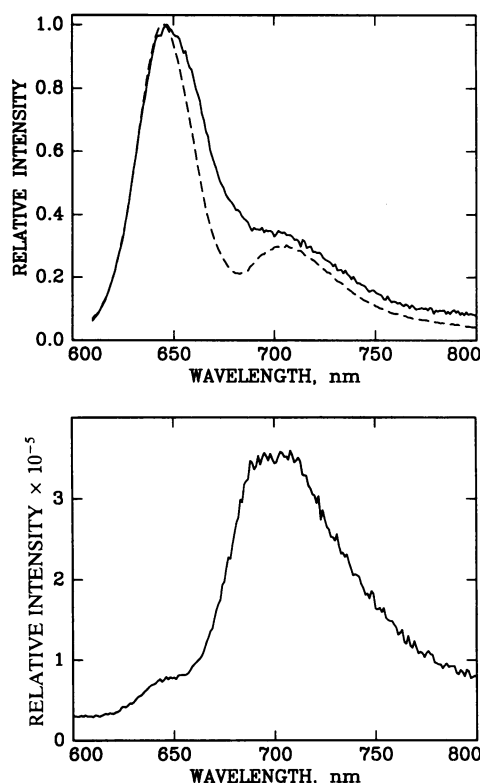


FIG. 2. Steady-state fluorescence spectra of membranes from TolE4B. (Upper) The spectra are normalized. The excitation wavelength was 600 nm. —, Absorbance at 678 nm is 0.3; ---, absorbance at 678 nm is 0.9. (Lower) The excitation wavelength is 450 nm. Absorbance at 678 nm is 0.3.

phycobiliprotein noticeable in the absorption spectrum, which is consistent with a previous observation (11). Since the phycobilisomes in this strain are uncoupled from the Chl, they have a high quantum yield. There is a small but distinct peak at ≈ 703 nm at low concentration (absorbance at the Q_y peak position < 0.3). When the sample concentration is high, the fluorescence peak is significantly red-shifted because of reabsorption. The 703-nm feature implies that excitations in the PSI core antenna are efficiently trapped at the reaction centers. The fluorescence spectrum with 450-nm excitation as shown in Fig. 2 Lower has no 680-nm peak ("bulk" fluorescence). Excitations at other wavelengths within the Soret bands yield similar results.

The ratio of Chl to P700, determined as described in text, is 130 ± 12 for the membranes suspended in HMCS (50 mM Hepes/5 mM $MgCl_2$ /5 mM $CaCl_2$ /1 M sucrose, pH 6.8), which is close to other intact preparations from cyanobacteria (120 Chls per P700) (23–26). Addition of Triton X-100 to the membrane preparation and chromatography of the detergent-treated membranes yielded a particle preparation free of carotenoids and phycobiliproteins with a Chl/P700 ratio of 60.

Fluorescence decay measurements were made on the two preparations described above. The data can be fitted to a sum of three exponentials with the lifetimes (τ) listed in Table 1. A dominant fast component (22 ps, 99.4%) indicates that the excitation is rapidly quenched in the reaction center, as tentatively concluded above. On the other hand, excitation at 630 nm and detection of the fluorescence decay from 650 to 680 nm reveals no fast components, confirming that in this region the absorption is dominated by the phycobiliproteins that have large fluorescence quantum yields. The column-purified PSI particles show the same fast component whether excited at 628 or 665 nm, indicating that the sample is free of phycobiliproteins (Table 2).

Table 1. Fluorescence decay parameters measured for a membrane sample in buffer

Excitation, nm	Emission, nm	τ_1 , ps	α_1 , %	τ_2 , ps	α_2 , %	τ_3 , ps	α_3 , %
630	650	257	23.0	1089	24.0	1626	43.0
	660	269	22.0	1169	45.0	1729	33.0
	670	237	27.0	1171	49.0	1863	24.0
	680	105	61.0	1053	26.0	1866	13.0
650	680	25.1	98.3	718	0.7	2198	1.0
	690	22.2	99.4	673	0.2	1909	0.4
	700	26.2	99.6	1483	0.2	1741	0.2

Since our result is close to the instrument limit of the single-photon counting setup, a fluorescence up-conversion experiment (4) with 650-nm excitation, 720-nm detection, and 150-fs pulse duration was performed with a membrane preparation. The fast component decay time obtained was 25 ± 2 ps (data not shown). This result gives us confidence that, for a decay dominated by a 25-ps component, our instrument response is adequate.

DISCUSSION

Due to gene deletions and interruptions, the *Synechocystis* mutant TolE4B contains neither PSII reaction centers nor PSII antennae. The protein that links phycobilisomes to the PSII centers is also gone. However, the PSI core antenna remains intact. Thylakoid membranes from TolE4B contain only the PSI core antenna as a Chl-containing component. The absorption and steady-state fluorescence emission characteristics of TolE4B membranes indicate the presence of a small amount of phycobiliproteins loosely associated with the membranes. However, this small number of phycobiliproteins does not seem to affect either the integrity of the PSI core antenna–reaction center complexes or the Chl-a fluorescence decay kinetics measured for the PSI complexes. The phycobiliproteins are energetically decoupled from the PSI core: energy transfer from them to the PSI core proceeds on a much slower time scale than the time scale on which excitation equilibration and trapping in PSI occur.

One of the fundamental issues regarding PSI is whether there exist red Chls around the reaction centers (8, 9, 23). Temperature dependence of energy transfer in PSI can be modeled successfully only when a few red pigments are included (8, 9). The fluorescence at 703 nm cannot originate directly from the bulk Chl molecules in the PSI core antenna, because the separation between the absorption peak of the antenna Chl (678 nm) and the steady-state fluorescence maximum (703 nm) is larger than the Stokes shift [normally < 14 nm for Chl-a in organic solvents (27)]. If such red pigments exist in TolE4B, the red-shifted fluorescence could be attributed to emission from them. Until recently, red-shifted steady-state fluorescence was observed for PSI preparations only at low temperatures. However, for PSI core particles with antenna size of 100 Chl per P700, from the cyanobacterium *Synechococcus*, Holzwarth and co-workers show an even more red-shifted emission at room temperature (10, 23).

Table 2. Fluorescence decay parameters for a particle sample prepared by hydroxylapatite column chromatography

Excitation, nm	Emission, nm	τ_1 , ps	α_1 , %	τ_2 , ps	α_2 , %	τ_3 , ps	α_3 , %
628	680	26.7	91.2	584	2.0	4393	6.8
	690	22.7	95.0	548	1.5	4009	3.5
665	680	17.7	94.1	651	0.9	4718	5.0
	690	22.4	96.6	491	0.4	4706	3.0
	700	28.1	94.8	508	1.2	4165	4.0

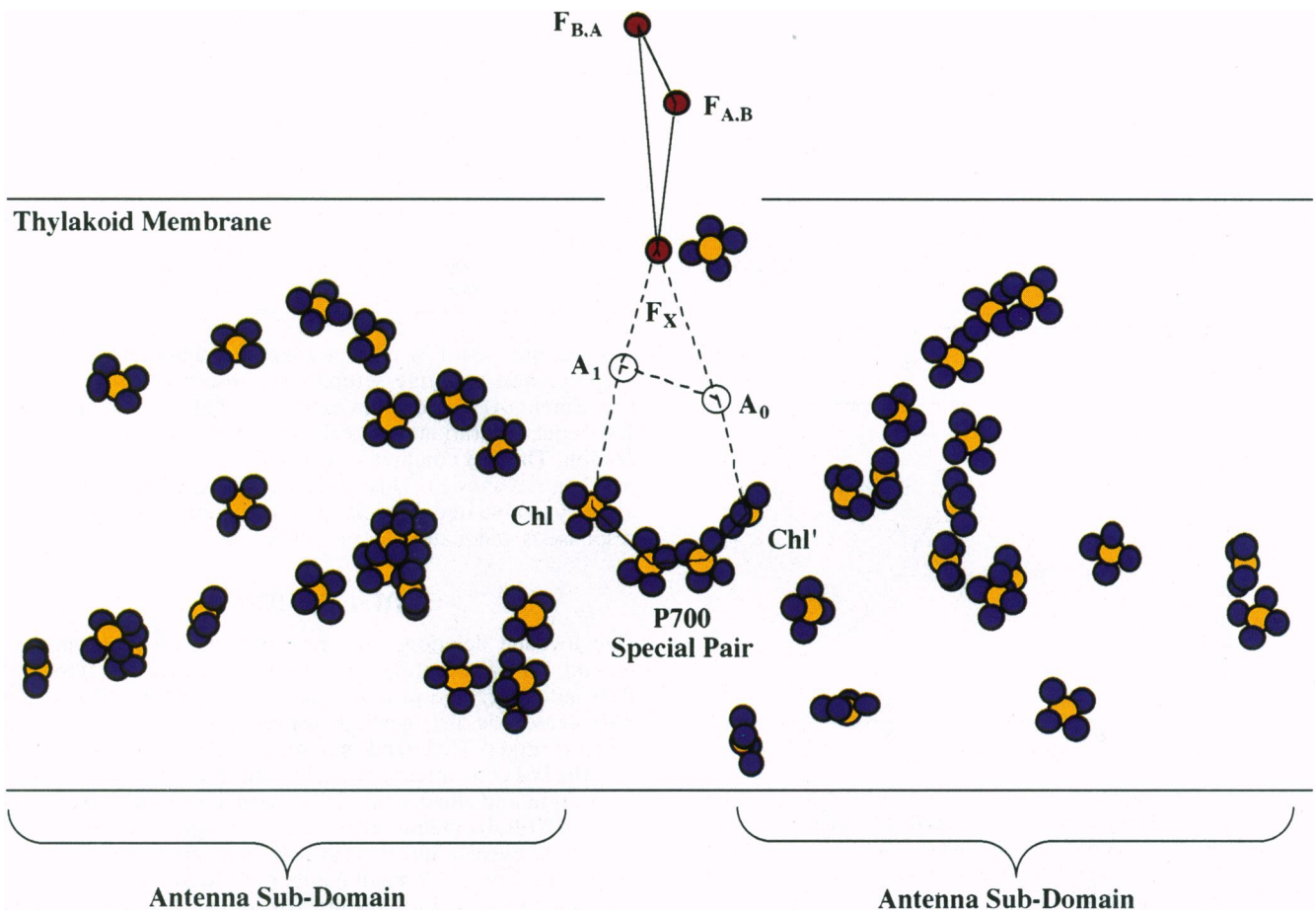


FIG. 3. The structure of PSI antenna. Each Chl-a is represented by five filled circles. Three iron atoms (single filled circles) are included to show the orientation of the structure. Chls are grouped into two domains. There is no communication between them except near the reaction center. The effective domain size is about half of the antenna. Positions of Chl and the reaction center components were taken from ref. 1.

Efficient energy transfer and trapping can be more directly studied by fluorescence decay measurements. The fact that the fluorescence decay from TolE4B membranes suspended in buffer solution is dominated (>98%) by a short decay component (lifetime, ≈ 25 ps) indicates that almost all of the chlorophyll pigments in the PSI core antenna of TolE4B are well connected to each other and to the reaction center. Previous studies of excitation trapping dynamics in PSI used samples from the green alga *C. reinhardtii* (5, 9, 28) and higher plants (24). Fluorescence decays from *C. reinhardtii* strain A4d, which is PSII-deficient, contain a long lifetime component (1–2 ns), which contributes from 5% to 15% to the initial amplitude. This decay component has been attributed to fluorescence from pigments not energetically coupled to a functional trap. The origin, location, and significance of these uncoupled Chls are still unclear. In addition to the long lifetime component, the fluorescence decay from A4d contains an intermediate component with a lifetime in the range of 100–700 ps and amplitude ranging from 5% to 30%. The origin of the intermediate component is not definitively assigned but is usually attributed to energy migration from peripheral antenna complexes to the core. Charge recombination in the reaction center has also been suggested as an alternative source of the intermediate decay component. But these two explanations do not account for the results reported here or those obtained by Hastings *et al.* (15). Therefore, we attribute the intermediate lifetime component to partially decoupled Chls and suggest that the charge separation in PSI is irreversible. Two features of PSI are consistent with greater irreversibility than that seen in PSII reaction centers: (i) P700 is a deeper energy trap than P680; (ii) the secondary electron

transfer is faster in the PSI reaction center than it is in the PSII reaction center (refs. 29 and 30; N. White, G. S. Beddard, and P. Heathcote, unpublished data).

A detailed understanding of the transfer of excitation energy to the reaction center requires a knowledge of PSI structure including the positions and orientations of the antenna pigments and the reaction center. Even when structural information is available, molecular models are still needed to account for the spectral-spatial relationships in PSI. Applications of simple lattice models have yielded microscopic energy transfer and trapping parameters (5). Numerical simulations designed to mimic an inhomogeneously broadened PSI system have accounted for the temperature dependence of fluorescence decay kinetics (8). We now apply this admittedly crude model to PSI with the goal of understanding why the steady-state fluorescence of TolE4B peaks around 700 nm and why the energy transfer is so efficient in PSI.

Constrained by a 25-ps trapping time, the simulation using a lattice of 130 Chls yields a charge separation time constant of ≤ 1 ps. The red fluorescence observed in our steady-state spectra can be simulated with a completely numerical approach including four red pigments and is not sensitive to the charge separation time constant over the range of 0.3–3 ps. Fluorescence peaking at 718 nm (10) can be simulated only when a significant number (more than eight) red Chl-a molecules are included along with a large fluorescence Stokes shift. The major factor keeping the fluorescence maximum in the 695- to 705-nm range is uphill energy transfer. Without the uphill energy-transfer process, our set of spectral types give a fluorescence spectrum peaking at 720 nm. The difference between our steady-state fluorescence result and that of others

(10, 23) may reflect the possibility that there are different numbers of red pigments or different Stokes shifts in other species.

It should be noted that the ≈ 1 -ps charge separation time obtained in the simulation is consistent with recent work of White *et al.* (N. White, G. S. Beddard, and P. Heathcote, unpublished data) but is inconsistent with the 3- to 4-ps charge separation time estimated by us previously (5) and with a recent measurement, in which a reaction center preparation with 12 Chls per P700 is used (29). We found that a 3- to 4-ps charge separation time is obtained in the simulation *only* when the number of Chls in each spectral type is reduced by half with the same spectral and spatial conditions. This suggests that the PSI system may contain two similar subantennae (domains), each having ≈ 65 Chls. This can occur, for example, if excitations can migrate freely within each domain and communication between domains occurs only in the vicinity of the reaction center.

The recent determination of the x-ray structure of PSI (1) provides us with an opportunity to relate the observed energy-transfer kinetics to the organization of the antenna pigments. In this crystallographic study, about half of the total Chl-a molecules in the PSI antenna were located. The antenna Chl-a molecules are associated with two protein subunits with transmembrane helical cores. The center-to-center distance between neighboring Chl-a molecules ranges from 8 to 15 Å. The electron-transfer chain is clearly shown to contain a P700 reaction center (a dimer of Chl-a), two Chl-a molecules (A_0 , A_1) and three iron-sulfur complexes (F_X , F_A , and F_B). Further, there exists a local pseudo-twofold axis that relates the two subunits of the transmembrane helical cores. The identified antenna Chl-a molecules (Fig. 3), which are arranged around the two protein subunits, apparently form two domains with a large spatial separation between them. The electron carriers are located between the two Chl pools. Thus, PSI may be divided into two subdomains that serve to funnel excitation energy to a single reaction center. The effective size of the PSI core antenna would then be about half the number of the total Chl-a molecules present in the antenna complex, which is consistent with our kinetic and lattice modeling results.

We found the Chl/P700 ratio for TolE4B membranes (in buffer solution) to be 130. In the presence of Triton X-100, the ratio reduces to about 60. The fluorescence lifetime of the fast decay component (≈ 25 ps) was not significantly altered by the detergent treatment. This observation is puzzling, but it has a number of possible explanations. (i) If the detergent penetrates into the PsaA and PsaB proteins, Chls can be stripped out randomly. The average distance between Chls would increase, while the total number of Chls would decrease. By coincidence, the overall effect due to slowing of the single-step transfer rate and reduction of the antenna size could result in little change of the lifetime. (ii) The Chls far from P700 have fewer connections to other Chls, and thus excitation leaves them and does not return. In this case, these "provincial" Chls would have little influence on the lifetime, which would be determined by the inner Chls. If detergent strips only outer Chls, it would have little effect on the overall trapping time. (iii) The detergent creates a wide distribution of antenna sizes, and our measurement is biased toward the results from subpopulations having larger antennae.

CONCLUSIONS

We modified an earlier lattice model to simulate energy transfer and trapping kinetics in PSI. The 25-ps fluorescent decay time for PSI in the thylakoid membranes of TolE4B leads us to calculate a ≤ 1 ps charge separation time constant by assuming a single antenna domain and a 3- to 4-ps charge

separation time constantly assuming two antenna domains. As improved structural information becomes available, we should be able to assess these alternatives by more realistic simulations and discriminate between the conflicting charge separation rates (refs. 29 and 30; N. White *et al.*, unpublished data). We do not observe an intermediate lifetime component for our samples. Such a lifetime is indicative of a partially disconnected antenna; its absence indicates that our sample is intact and that irreversible charge separation occurs in PSI.

This work was supported by research grants from the International Human Frontiers of Science to R.H. and from the National Science Foundation to G.R.F. L.D.M. was a predoctoral trainee in Molecular Biophysics (National Institutes of Health Grant GM 08282). J.R.N. held a research fellowship from the Amoco Foundation (Grant 930096).

1. Krauss, N., Hinrichs, W., Witt, I., Fromme, P., Pritzkow, W., Dauter, Z., Betzel, C., Wilson, K. S., Witt, H. T. & Saenger, W. (1993) *Nature (London)* **361**, 326–331.
2. Golbeck, J. H. (1987) *Biochim. Biophys. Acta* **895**, 167–204.
3. Lagoutte, B. & Mathis, P. (1989) *Photochem. Photobiol.* **49**, 833–844.
4. Du, M., Xie, X., Jia, Y., Mets, L. & Fleming, G. R. (1993) *Chem. Phys. Lett.* **201**, 535–541.
5. Owens, T. G., Webb, S. P., Mets, L., Alberte, R. S. & Fleming, G. R. (1987) *Proc. Natl. Acad. Sci. USA* **84**, 1532–1536.
6. Pearlstein, R. M. (1982) in *Photosynthesis*, ed. Govindjee (Academic, New York), pp. 293–330.
7. Pearlstein, R. M. (1982) *Photochem. Photobiol.* **35**, 835–844.
8. Jia, Y., Jean, J. M., Werst, M. M., Chan, C.-K. & Fleming, G. R. (1992) *Biophys. J.* **63**, 259–273.
9. Werst, M. M., Jia, Y., Mets, L. & Fleming, G. R. (1992) *Biophys. J.* **61**, 868–878.
10. Holzwarth, A. R., Schatz, G., Brock, H. & Bittersmann, E. (1993) *Biophys. J.* **64**, 1813–1826.
11. Woolf, V. M., Wittmershaus, B. P., Vermaas, W. F. J. & Tran, T. D. (1994) *Photosynth. Res.* **40**, 21–34.
12. Shiozawa, J. A., Alberte, R. S. & Thornber, J. P. (1974) *Arch. Biochem. Biophys.* **165**, 388–397.
13. Bengis, C. & Nelson, N. (1975) *J. Biol. Chem.* **250**, 2783–2788.
14. Mullet, J. E., Burke, J. J. & Arntzen, C. J. (1980) *Plant Physiol.* **65**, 814–822.
15. Hastings, G., Kleinherenbrink, F. A. M., Lin, S. & Blankenship, R. E. (1994) *Biochemistry* **33**, 3185–3192.
16. Herdman, M., Delaney, S. F. & Carr, N. G. (1973) *J. Gen. Microbiol.* **79**, 233–237.
17. DiMagno, L. (1992) Ph.D. thesis (Univ. of Chicago, Chicago).
18. Rögner, M. D., Chisholm, D. A. & Diner, B. A. (1991) *Biochemistry* **30**, 5387–5395.
19. Ray, W. J. & Puvathingal, J. M. (1985) *Anal. Biochem.* **146**, 307–312.
20. Hayama, T. & Ke, B. (1972) *Biochim. Biophys. Acta* **267**, 160–171.
21. Chang, M. C., Courtney, S. H., Cross, A. J., Gulotty, R. J., Petrich, J. W. & Fleming, G. R. (1985) *Anal. Instrum.* **14**, 433–464.
22. van Grondelle, R., Dekker, J. P., Gillbro, T. & Sundstrom, V. (1994) *Biochim. Biophys. Acta* **1187**, 1–65.
23. Turconi, S., Schweitzer, G. & Holzwarth, A. R. (1993) *Photochem. Photobiol.* **57**, 113–119.
24. Boekema, E. J., Dekker, J. P., Van Heel, M. G., Rögner, M., Saenger, W., Witt, I. & Witt, H. T. (1987) *FEBS Lett.* **217**, 283–286.
25. Hefti, A., Ford, R. C., Miller, M., Cox, R. P. & Engel, A. (1992) *FEBS Lett.* **296**, 29–32.
26. Golbeck, J. H. (1992) *Annu. Rev. Plant Physiol. Plant Mol. Biol.* **43**, 293–324.
27. North, A. M., Pethrick, R. A., Kryszewski, M. & Nadolski, B. (1978) *Acta Phys. Pol. A* **54**, 797–804.
28. Owens, T. G., Webb, S. P., Alberte, R. S., Mets, L. & Fleming, G. R. (1988) *Biophys. J.* **53**, 733–745.
29. Kumazaki, S., Kandori, H., Petek, H., Yoshihara, K. & Ikegami, I. (1994) *J. Phys. Chem.* **98**, 10335–10342.
30. Hastings, G., Kleinherenbrink, F. A. M., Lin, S., McHugh, T. J. & Blankenship, R. E. (1994) *Biochemistry* **33**, 3193–3199.